

Performance of Battery and SMES Based Dynamic Voltage Restorer to Enhance Voltage Sag in Grid Connected Hybrid PV-Wind Power System

Dr.RAMACHANDRA C G

PG Student, Dept of EEE, S V University College of Engineering, Tirupati.

Dr.NATHALIE JOHN

Assistant Professor, Dept of EEE, S V University College of Engineering, Tirupati.

ABSTRACT

To provide green energy, the renewable energy sources are most preferable choice in the world. Most of the Renewable energy sources especially Wind and Solar PV depends on wind speed and solar irradiance. Due to this limitation, they lead to power fluctuations. The dynamic voltage restorer (DVR) is used to protect and compensate the sensitive loads affected by load side fluctuations. This paper attempts to withstand and secure the effect of voltage fluctuations of grid connected hybrid PV-Wind power system. For voltage sag condition, a DVR with battery and super magnetic energy storage (SMES) is used as a compensating device. In this paper the pre-sag compensation is used for compensation which locks both magnitude and phase angle. The Park and inverse park transform techniques are used in the control of voltage source converter (VSC) of DVR. The compensation is carried out for both symmetrical and asymmetrical voltage sag cases by using MATLAB/SIMULINK software.

Keywords:Dynamic voltage restorer (DVR), Voltage source converter (VSC), Power quality, Voltage sag compensation.

1. INTRODUCTION

The energy consumption increased in the world due to increasing development of population of the world and also due to the large number of industrial plants. The energy consumption was nearly twice from the past five years [1]. The non-renewable energy sources like coal, oil and natural gas etc., are not suitable to meet these energy consumptions because its lack of probability in the nature, cost of the resources, capital investment and these produce greenhouse effect gases like carbon dioxide, methane and certain other gases in the air. So that, the renewable energy sources (RES) including PV solar, Wind energy, Geothermal energy, energy from the oceans and biomass energy are suitably used to meet these energy consumptions.

Renewable energy sources include both 'direct' solar radiation and 'indirect' solar energy mostly wind, tidal, wave and biomass energy resources that can be managed in a suitable manner. Among all RES, solar PV and wind energy sources are most used due to its availability to construct and extract.

The combination of renewable energy sources commonly PV solar and Wind system are connected to grid, it supplies the energy to different localities [4]. The power fluctuations occurred by the grid connected system due to dependence on weather conditions such as wind speed and solar irradiance [3], [4]. To reduce these fluctuations the compensation techniques should be implemented at the remote locations. The power fluctuations reduced to maintain within the limits can be done by using custom power devices (CPD). The CPD are connected either in series, or parallel or combination of both at the remote locations (or load end side). The CPD are static var compensator, distribution static compensator (DSTATCOM), active filters and dynamic voltage restorer (DVR) [5], [7].

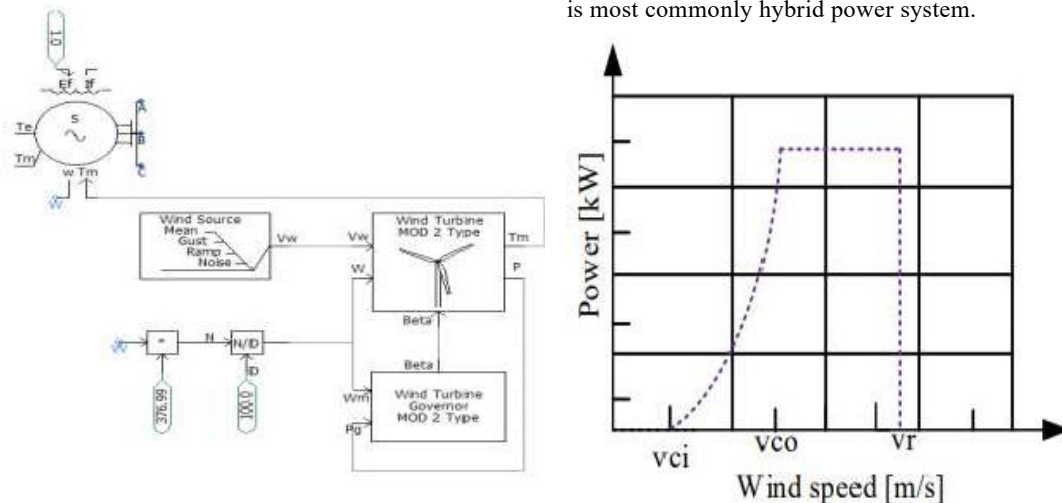
A series type DVR is one of the most used compensation techniques for the improvement of power quality problems such as sag, swell, harmonics, flickers and interruptions that can separate the consumer loads from the system to reduce the losses [5], [8]. Sag is the one of the most occurred in the system due to starting of large motors, switching of power electronic devices, faults at the bus and burden on transformer. This can affect the magnitude and phase jumps [7]. The DVR stores the energy through capacitors and external devices nearly battery energy storage (BES) and super magnetic energy storage (SMES) [6], [9], [10]. The combined BES-SMES based DVR is used in the grid connected PV-Wind hybrid energy system for the improvement of voltage sag [6], [9], [11], [12].

During voltage sag conditions, the DVR will discharge and inject the voltage to compensate the missing voltage and during voltage swell conditions the DVR will charge and stores the energy in BES and SMES devices [11]. The SMES will be combined with BES to increase the performance of the DVR [6], [12]. The control and compensation techniques of DVR are described in [7]. The pre-sag compensation technique is used to lock the instantaneous voltage of three phase magnitude and phase angle jumps [6], [11].

The hybrid PV-Wind energy systems will not be stable and should not produce required output. The system will be stable and produce required output attained by using HES based DVR with BES and SMES devices. The disturbances in the system are mainly due to non-linear power output of renewable energy sources of PV and Wind energy systems. The operation of DVR for improving the voltage sag is done by MATLAB/SIMULINK software. HES to grid connected is described in section 2. The proposed DVR with BES-SMES based HES is described in section 3. The FUZZY logic controller described in 4. Results of simulation and conclusion are described in section 5 and 6.

2. HYBRID PV-WIND POWER SYSTEM TO GRID CONNECTED

The renewable energy sources like Wind and PV energy sources are naturally comfortable in environment and gradually reduces its investment costs [2], [13]. The total installed capacity of solar PV and Wind energy systems are more than 405GW [15] and 539GW [14]. The solar PV and Wind systems depends on irradiance and wind speed data [3], [14], [15]. The wind turbine system and its power curve is shown in fig. 1 [1], [14], [16]. The wind turbine output power (P_{WT}) is determined using the equation (1). As shown in the power output of wind turbine, the output power is non-linear and non-zero values from the interval cut-in to rated wind speed values. To provide constant output power to load end consumers it should be combined with another renewable energy sources like solar PV which is most commonly hybrid power system.



a) Wind turbine system

Figure 1. Wind turbine system and its power curve

$$P_{WT}(V) = \begin{cases} 0, & 0 < V < V_{ci} \\ 0.5\rho A V^3 C_p, & V_{ci} \leq V < V_{co} \\ 0.5\rho A V_r^3 C_p, & V_r \leq V < V_{co} \\ 0, & V \geq V_{co} \end{cases} \quad \dots\dots\dots (1)$$

Where V_{ci} is cut-in speed, V_r is rated wind speed, V_{co} cut-out speed, A is swept area, ρ air density and C_p is the power co-efficient of wind system.

The equivalent circuit of a PV cell and its power output curve is as shown in fig. 2 [2], [17]. The output of a PV cell is DC which is converted to AC using inverter to grid connected. The maximum power

output of a cell is calculated using equation (2). Maximum power point tracking (MPPT) control technique is used to get maximum output from the PV cell [13], [17], [18]. The open circuit voltage (V_{oc}) and short circuit current (I_{sc}) are determined from (4) and (5) depends on irradiance and temperature of a PV cell.

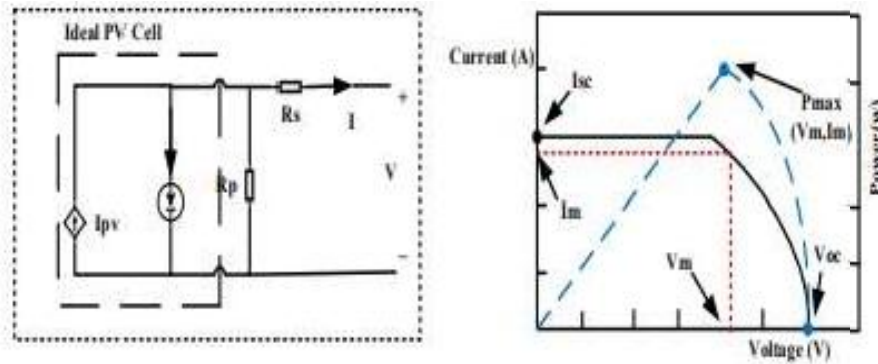


Figure 2. PV circuit and its curve

$$P_{max} = V_{oc} \cdot I_{sc} \cdot FF \dots \dots \dots (2)$$

Where P_{max} is maximum output power, V_{oc} is open circuit voltage, I_{sc} is short circuit current of a PV cell and FF is fill factor.

$$\text{Where, } FF = \frac{V_m I_m}{V_{oc} I_{sc}} \dots \dots \dots (3)$$

$$V_{oc} = V_{oc}^* + \beta_v (T - 25) \dots \dots (4)$$

Where V_{oc}^* is PV cell open circuit voltage under standard test conditions, β_v temperature co-efficient regarding open circuit voltage, T is temperature of the cell.

$$I_{sc} = \frac{G}{G_n} (I_{sc}^* + \beta_i (T - 25)) \dots \dots (5)$$

Where I_{sc}^* is PV cell short circuit current under standard test conditions, β_i temperature co-efficient regarding short circuit current, G is incident solar irradiance and G_n is incident solar irradiance under standard test conditions.

$$P_{PV} = P_{STC} \frac{G}{G_n} (1 - \gamma(T - 25)) \dots \dots (6)$$

Where P_{STC} is maximum output power under standard test conditions, γ is temperature co-efficient to maximum power.

$$T = T_{amb} + \frac{G}{G_{NOCT}} (G_{NOCT} - T_{NOCT}) \dots \dots (7)$$

Where T_{amb} is ambient temperature, G_{NOCT} is incident irradiance under normal operating temperature.

On-grid hybrid PV-Wind power system is as shown in the fig. 3 [17]. It is consisting of PV solar, wind turbine system and grid main low voltage. To provide voltage to power distribution loads these are connected to PCC bus. During steady state conditions a constant voltage of 5kV is supply to the PCC bus through wind, solar and low voltage grid line. During any disturbances like faults, it supplies above or below 5kV to the PCC bus. The distribution loads affected by voltage fluctuations can be withstand by using custom power devices.

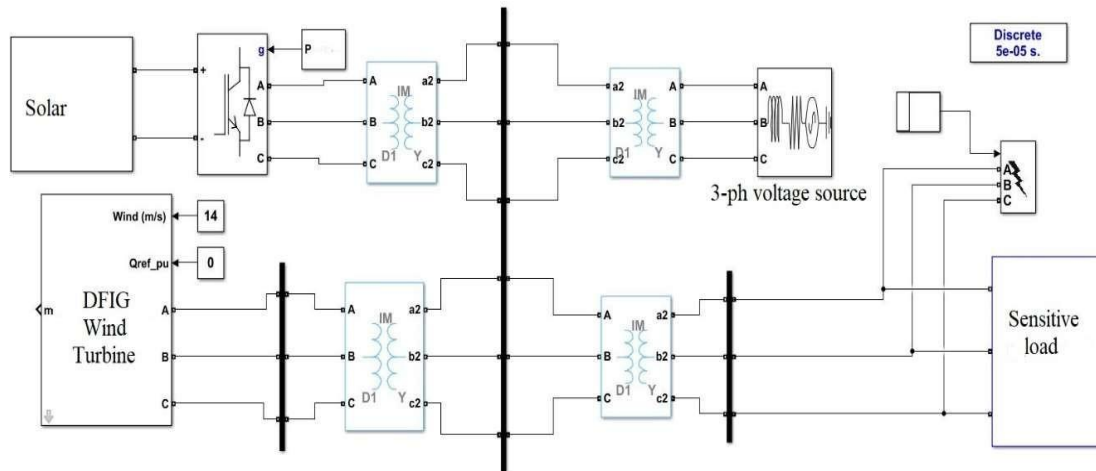


Figure 3. Hybrid PV-Wind power system

3. DVR WITH BES-SMES BASED HES

The SMES can store the energy in the of electromagnetically and BES can store the energy in the form of electrochemically because an AC system cannot store energy electrically. To improve the power quality, custom power devices are the most preferable choice [10]. In case of voltage swell conditions, the SMES will charge, and it can be released during voltage sag conditions to maintain load voltage as stable [19]. During charging the SMES will act as an inductive load and during discharging state it acts as a reducible current source [6], [19]. To increase the response time combination of BES and SMES devices to withstand the voltage fluctuations affected by the distribution loads [2].

The grid connected hybrid PV-Wind with BES and SMES based DVR system and its detailed block diagram is shown in fig. 4 and fig. 5 and its parameters are described in Table 1.

Table (1): Grid connected Hybrid system

Parameters	Value
PV source voltage stepup	1kV/5kV, 60Hz
Grid line voltage step down	11kV/5kV, 60Hz
PCC bus voltage	5kV
Load side Transformer	5kV/0.48kV, 60Hz
Load capacity	0.1MW+0.1MVar

To determine any disturbance or fault and reference signal is a basic need to control the DVR system [20]. To identify the voltage sag or swell conditions we need to determine the real time three phase instantaneous voltage at PCC bus and evaluate with the root mean square per unit voltage (V_{pu}) to observe the any interruption or fault. The generation of reference signal is a type of compensation technique is used. The compensation techniques are pre-sag, in-phase, energy optimized and hybrid compensation. In Case of voltage dips (sag condition) the DVR will inject the voltage to compensate the voltage dips and during voltage spikes (swell condition) the DVR will absorb excess voltage and it can be stored in hybrid energy system. Proper operation of DVR will be done through controlling of BES, SMES and VSC is as shown in the fig. 6, fig. 7, fig. 9 and the related parameters mentioned in Table 2.

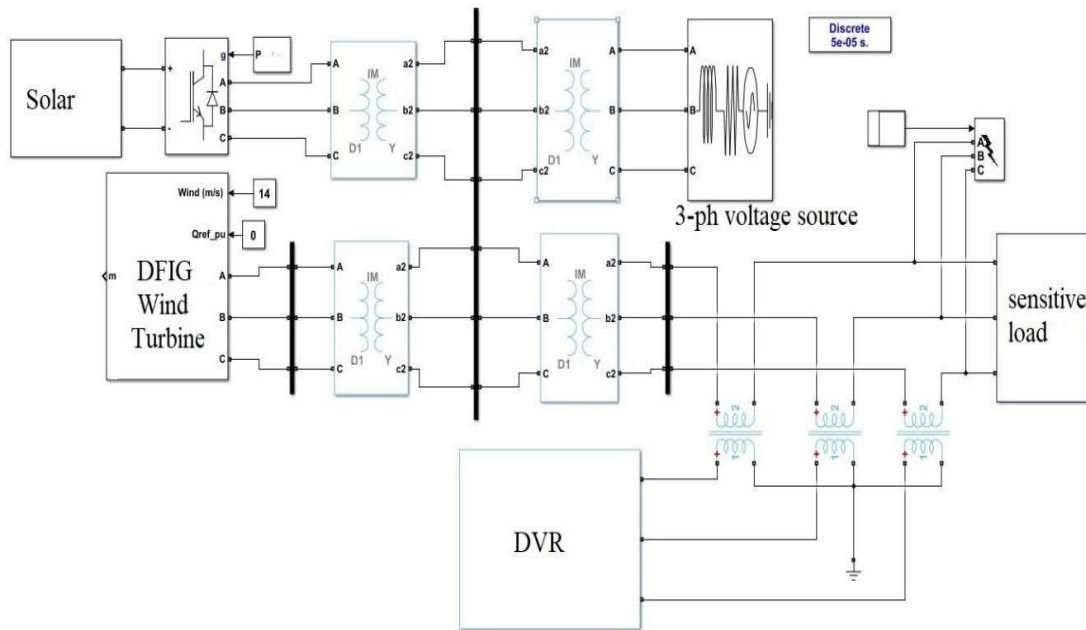


Figure 4. The proposed BES-SMES based DVR

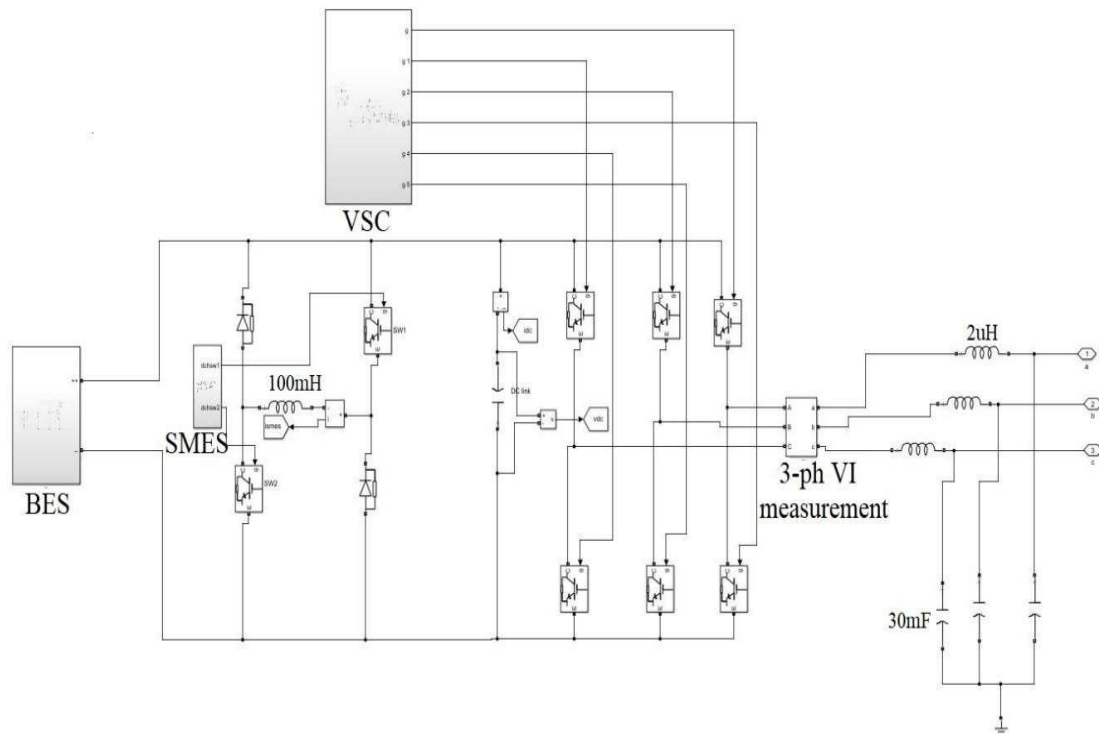


Figure 5. Detailed block diagram of BES-SMES based DVR

The control block diagram of BES is shown in fig. 5, the degree of voltage level at the point of common coupling (PCC) and the battery state of charge (SOC), the battery will be charged or discharged or with in the energy storing conditions. The state of charge is in the interval between 5% and 100% to limit the damage of battery from excess charging and discharging conditions.

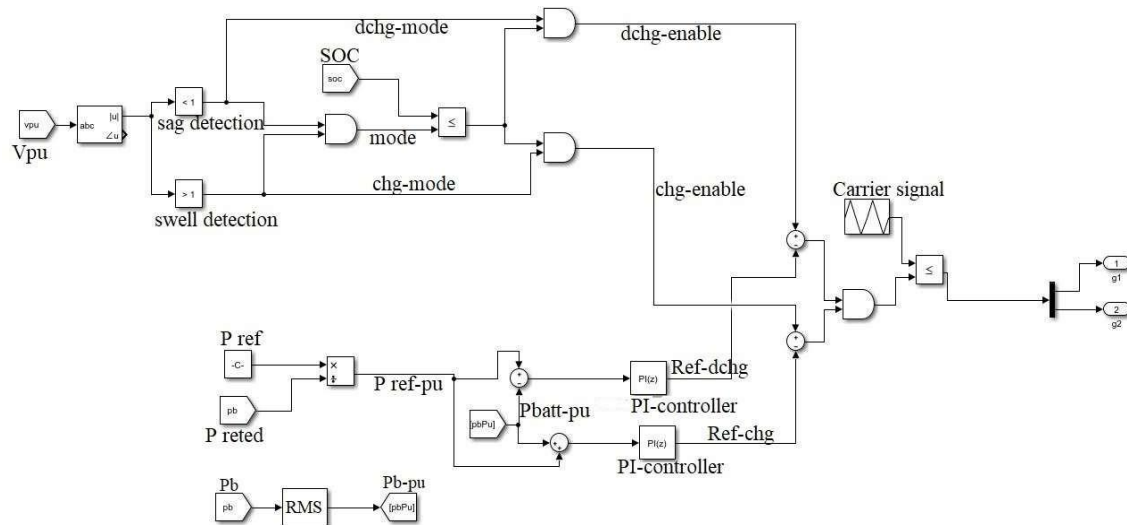


Figure 6.BES Control block diagram

The control block diagram of BES is shown in Fig. 6, by observing the status of ON switch, the charging and discharging switches will charge and discharge the BES. If SOC will cross the limits, then the SOC signal will not allow for charging and discharging conditions. To get per unit value of reference power, the reference power is considered and compared with rated capacity of battery. For the generation of reference discharge signal (Ref-Discharge), the error will be passes through PI controller1. To generate reference charging signal (Ref-Charge), reference per unit value add with battery per unit value and that can be passes through PI controller2. The carrier signal of frequency 5kHz will be compared with reference signals to get the gate pulses of charging and discharging conditions.

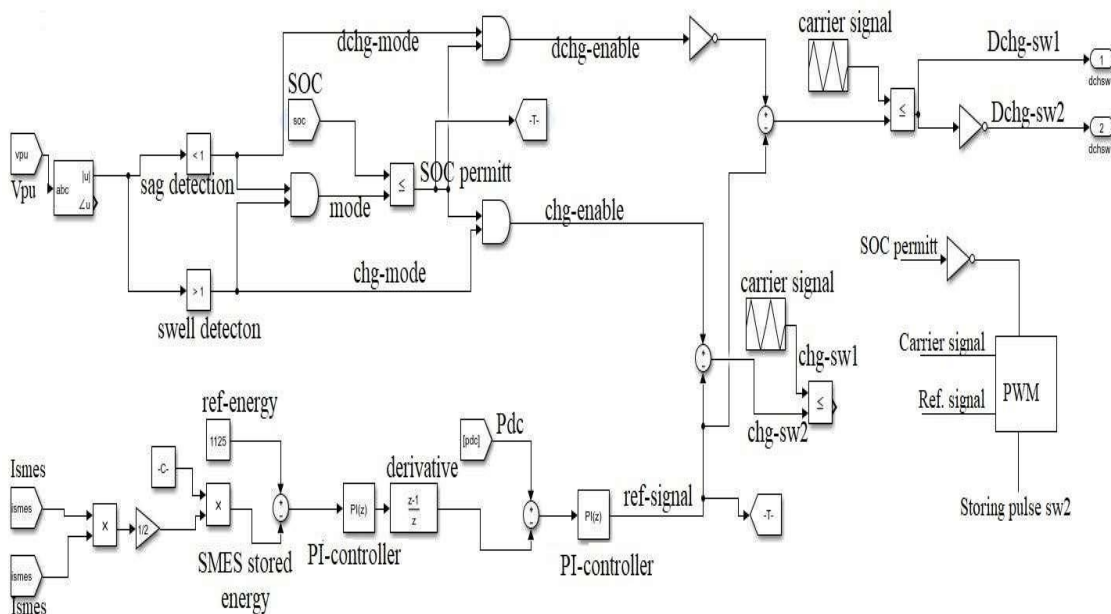


Figure 7.SMES Control block diagram

The control block diagram of SMES is shown in fig. 7, the degree of voltage level at the point of common coupling (PCC) and the SMES state of charge (SOC), the SMES will be charged or discharged or with in the energy storing conditions. If both switches sw1 and sw2 are ON, then the SMES will be in charging condition. The SMES will be in discharging condition, if both switches sw1 and sw2 will be OFF. If either

switches sw1 or sw2 will be turned ON and another will be OFF, then the SMES will be under energy storing condition.

Table (2): specifications of BES-SMES HES based DVR

Parameters	Value
Filter inductance	2 μ H
Filter capacitance	30mF
DC-link capacitance	55mF
DC-link rated voltage	500V
SMES inductance	0.1H
SMES critical current	150A
BES capacity	200Ah
Battery nominal voltage	600V
Injection transformer rating	0.48kV/0.48kV, 60Hz

The reference energy is compared with SMES stored energy, and it can be sent to PI controller. The controller output multiplied with ON or OFF value and that can be sent to differentiator to get power. Later, the DC power in DC-Link capacitor compared with SMES power and it can be multiplied with ON or OFF value, that will be passes to PI controller to get reference signal. Similarly, BES the SMES will charge and discharge if it's SOC below 100% and above 5%.

The charging, discharging and energy storing conditions of BES and SMES, the total combination of BES-SMES based DVR will be operated.

The different voltage sag compensation techniques are pre-sag, in-phase and energy optimized techniques are as shown in fig. 8 and are described [6], [7] and [16].

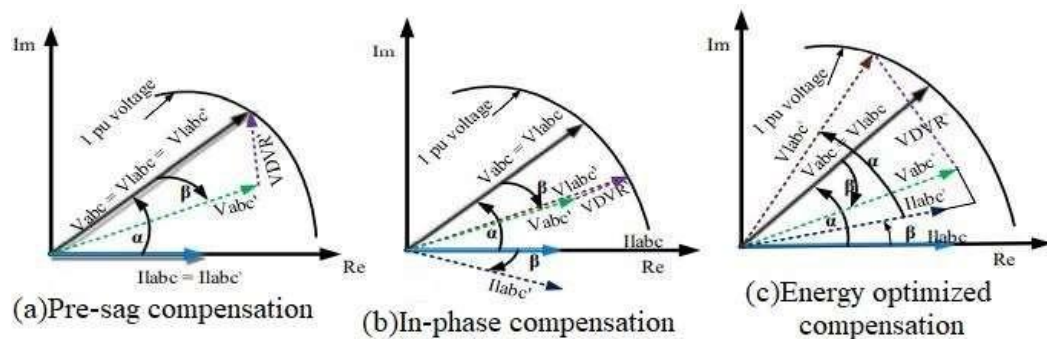


Figure 8.DVR voltage compensation techniques

In this, the pre-sag compensation technique is used for the recovery of sag and swell voltage magnitudes and phase angle jumps. This compensation technique is also used for non-linear thyristor-controlled loads to recover phase jumps still it consumes a part of extra active power from the DC-Link. [6], [7] and [16]. As shown fig. 8, V_{abc} is voltage magnitude of three phase line prior to fault and V_{abc}' is voltage magnitude of three phase line at the time of fault occurrence. V_{abc} is output voltage prior to fault, V_{abc}' is output voltage during the fault and V_{DVR} is DVR injected voltage at the time of fault occurrence. Similarly, I_{abc} is output or load current prior to fault and I_{abc}' is output or load current at the time of fault occurrence.

To modify the DC-Link voltage, direct axis current (id) and to modify the reactive power, quadrature

axis current (i_q) are used in the current controlled pulse width modulation (PWM) converter [21]. To regulate the active and reactive power transferred between the DC and AC sides of voltage source converter (VSC), the sinusoidal pulse width modulation (SPWM) technique and voltage control techniques are used in the controlling of VSC as shown in fig. 9.

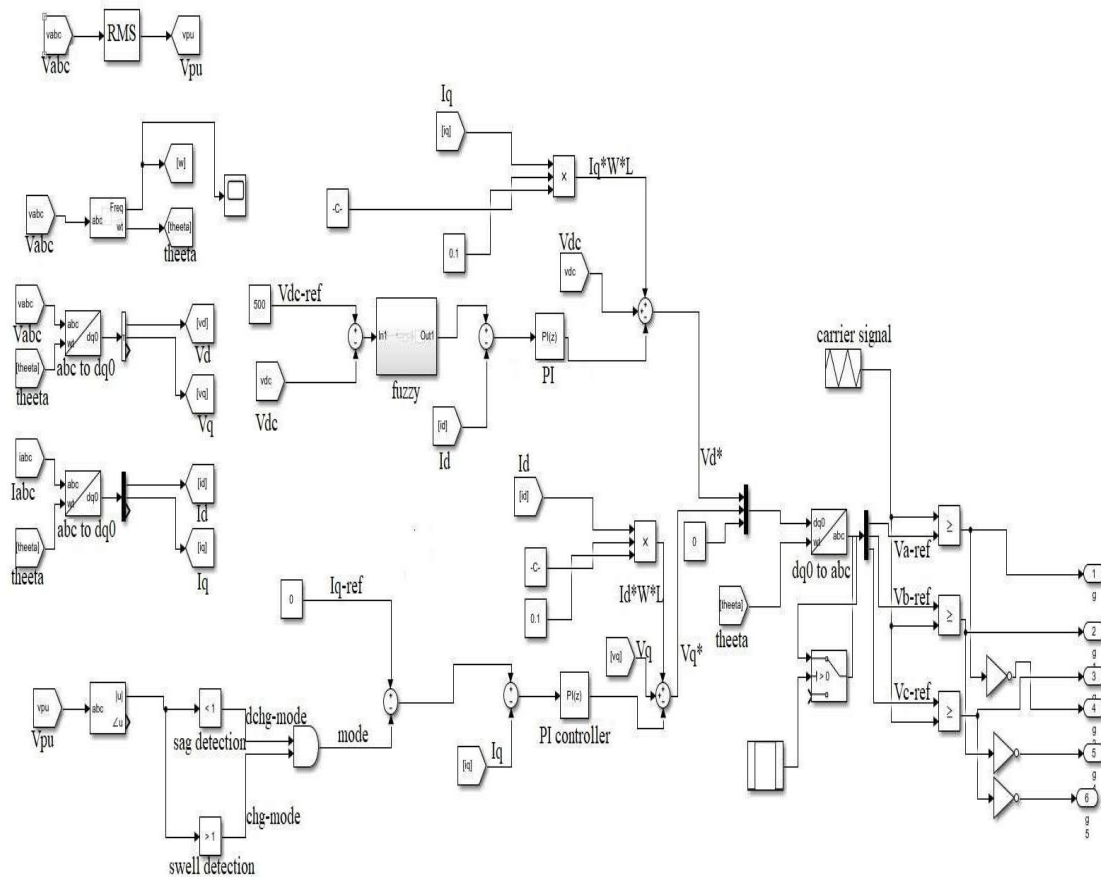


Figure 9. VSC Control block diagram

V_{abc} is converted into V_d and V_q elements when it is passed through transformation technique called as park transform. Similarly, I_{abc} is converted into I_d and I_q elements by applying park transform. These I_d and I_q are in-phase and perpendicular to the three-phase voltage V_{abc} . The active power exchange between AC and DC sides of VSC is done by using direct axis element, I_d and it can also control the voltage of DC-Link. Similarly, the reactive power component at the VSC terminals can be controlled by using quadrature axis element, I_q .

To produce the conjugate component of V_d , compares the components of V_d and $I_q \cdot W \cdot L$ where, $W = 2\pi f$ and L is inductance of SMES and to produce the conjugate component of V_q , compares the components of V_q and $I_d \cdot W \cdot L$. The elements of V_d^* and V_q^* are passed through transformation technique called as inverse park transform to obtain the modulations waveform signals $V_a\text{-ref}$, $V_b\text{-ref}$ and $V_c\text{-ref}$ signals as shown in fig. 9. The frequency value of 5040Hz triangular carrier signal is compared with modulation waveform signals to generate firing pulses.

4. FUZZY LOGIC CONTROLLER

Fuzzy logic system is a complex mathematical method to determine the different simulation problems with inputs given as error and change in error. The basic fuzzy logic system is as shown in fig. 10.

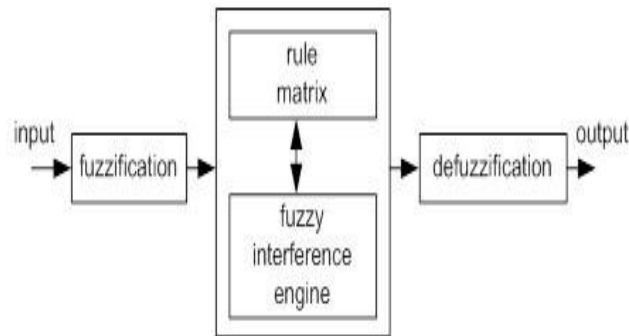


Figure 10. Fuzzy logic controller

The major components of fuzzy system is shown fig 10 [22]. are input variables, fuzzification interface, rule matrix, fuzzy inference engine, defuzzification interface, and output variables. First phase of fuzzy system is that the input variables given to fuzzification inference mechanism to produce output result. The fuzzy rules are interpreted in the rule matrix, which is a simple graphical representation toll to mapping the fuzzy rules [22]. The fuzzy rules and its rule matrix are as shown in Table 3. Membership functions, logical operations and if-then rules are described in fuzzy inference engine to mapping the given input to output. The main function of Defuzzification inference mechanism is to change the fuzzy output set into crisp output values. The various defuzzification techniques are centroid, mean, maximum and weighted average defuzzification techniques. Among all, the centroid technique is most commonly used defuzzification technique.

Table (3): Fuzzy logic controller rule

'e' 'ce'	NB	NM	NS	ZE	PS	PM	PB
NB	NB	NB	NB	NB	NM	NS	ZE
NM	NB	NB	NB	NM	NS	ZE	PS
NS	NB	NB	NM	NS	ZE	PS	PM
ZE	NB	NM	NS	ZE	PS	PM	PB
PS	NM	NS	ZE	PS	PM	PB	PB
PM	NS	ZE	PS	PM	PB	PB	PB
PB	ZE	PS	PM	PB	PB	PB	PB

The fuzzy rules are given to the fuzzy system are shown in Table 3. These rules are used by the fuzzy controller to produce required output. The membership functions for inputs error and change in error are shown in fig 11(a) and 11(b) and output membership function of input control change is shown in fig 11(c) [22].

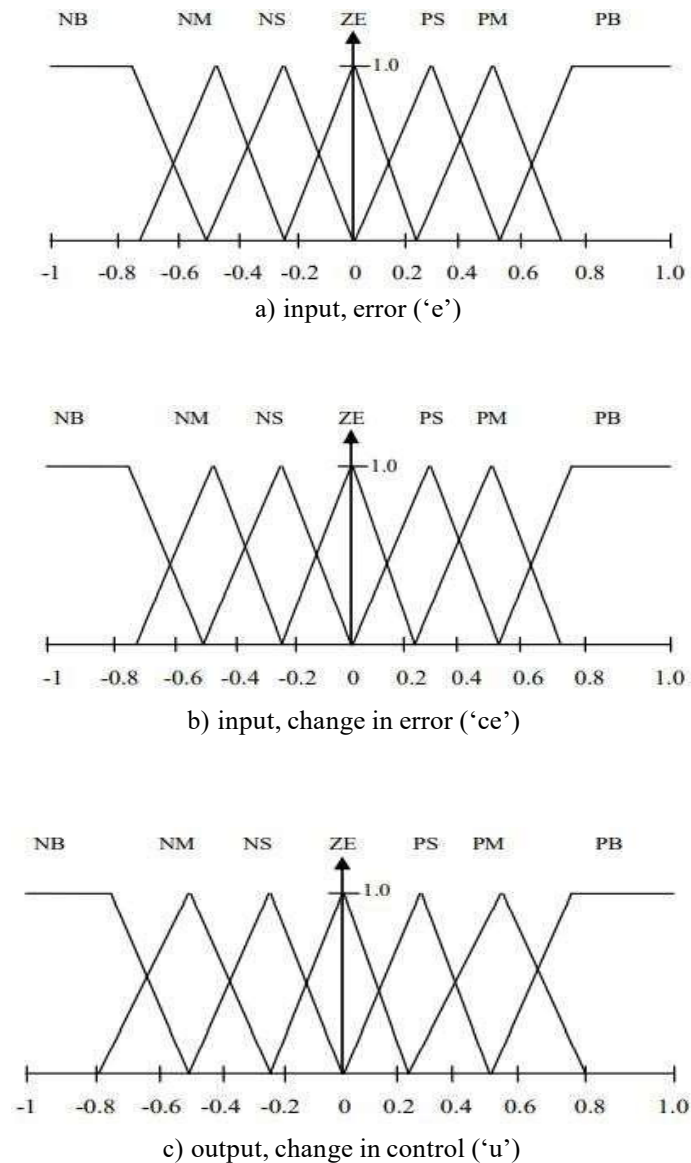
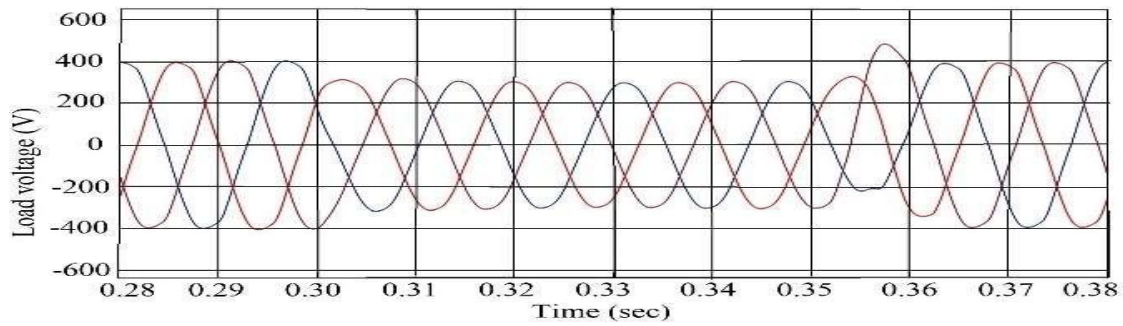


Figure 11. Fuzzy logic membership functions

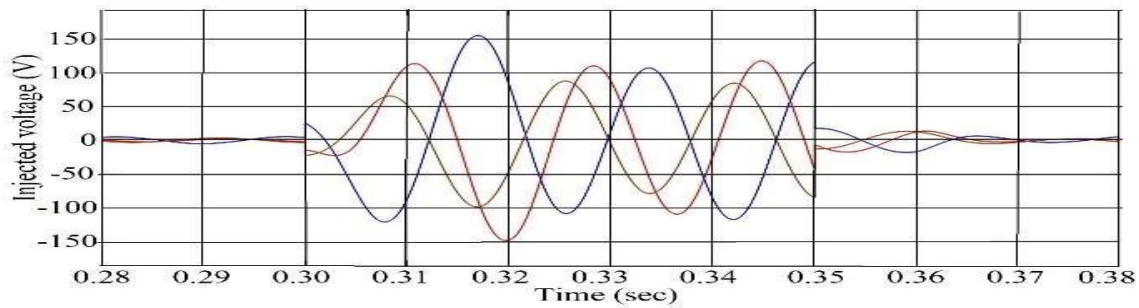
5. SIMULATION AND RESULTS

The operation of BES-SMES based dynamic voltage restorer (DVR) as shown in fig. 4 and the related parameter values mentioned in Table 2, the simulation is done for 50 milliseconds duration time by using MATLAB/SIMULINK software. Due to switching transients present in the system at the start and stop of DVR operation, very short time the simulation not completely compensated.

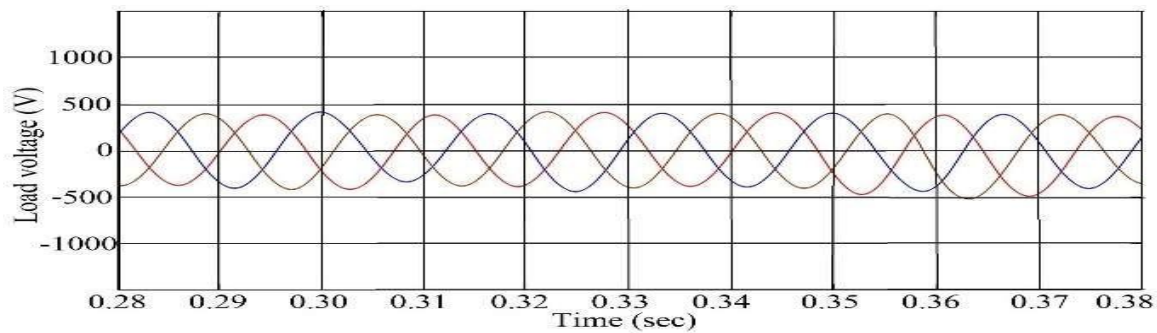
For symmetrical voltage sag case, as shown in fig 12(a) and fig 13(a), the load voltage without DVR dropped to 75% and 88% of rated value. After injecting DVR voltage as shown in fig 12(b) and 13(b), the load voltage is improved to normal value as shown in fig 12(c) and 13(c). Similarly for asymmetrical voltage sag case, as shown in fig 14(a) and fig 15(a), the load voltage without DVR dropped to 75% and 65% of rated value. After injecting DVR voltage as shown in fig 14(b) and 15(b), the load voltage is improved to normal value as shown in fig 14(c) and 15(c).



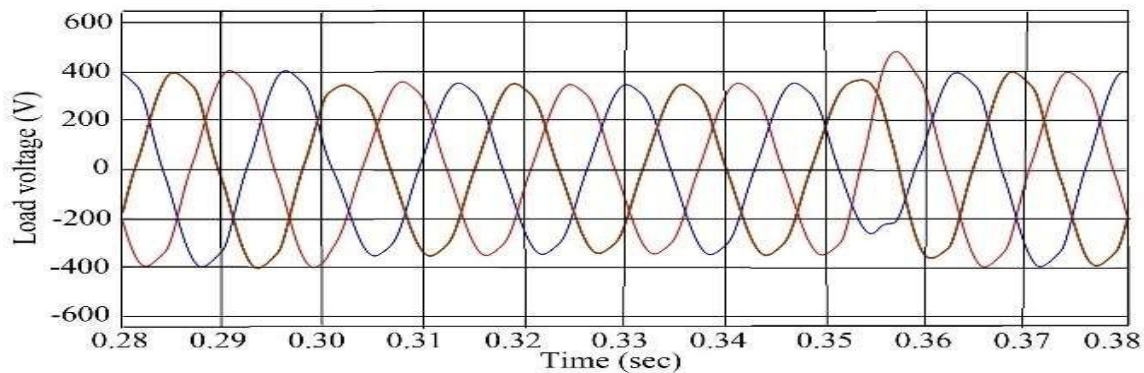
12(a) Load voltage without DVR



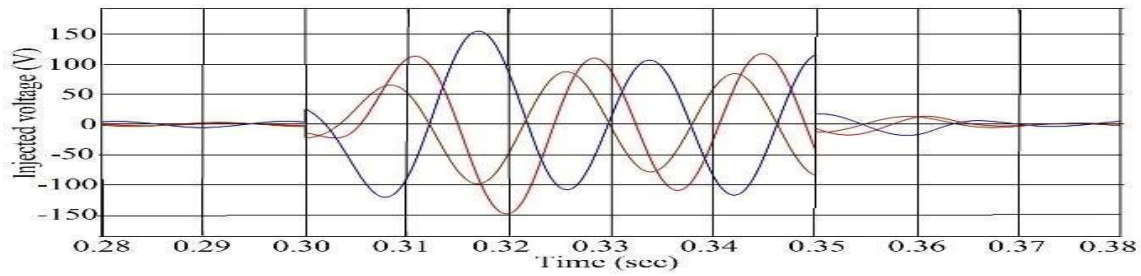
12(b) Injected voltage of DVR



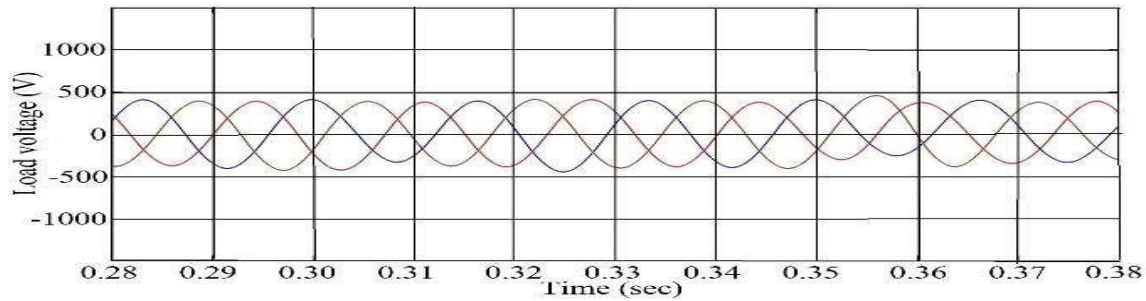
12(c) Load voltage with DVR

Figure 12.25% symmetrical voltage sag case response of DVR

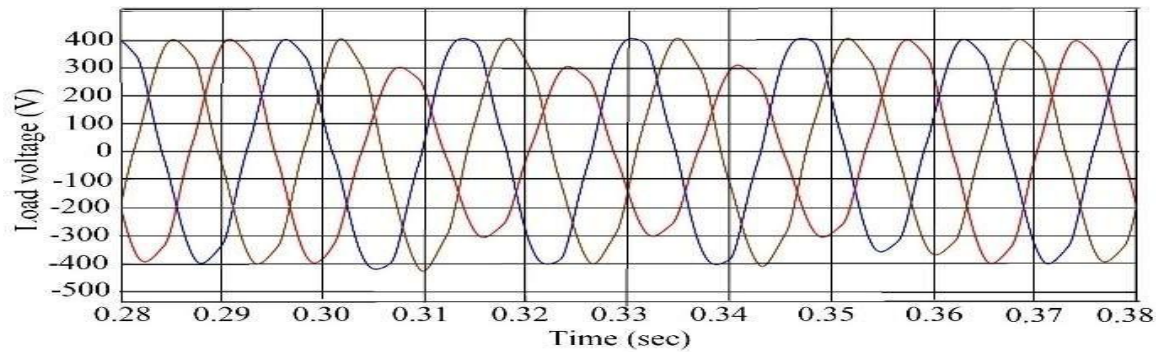
13(a) Load voltage without DVR



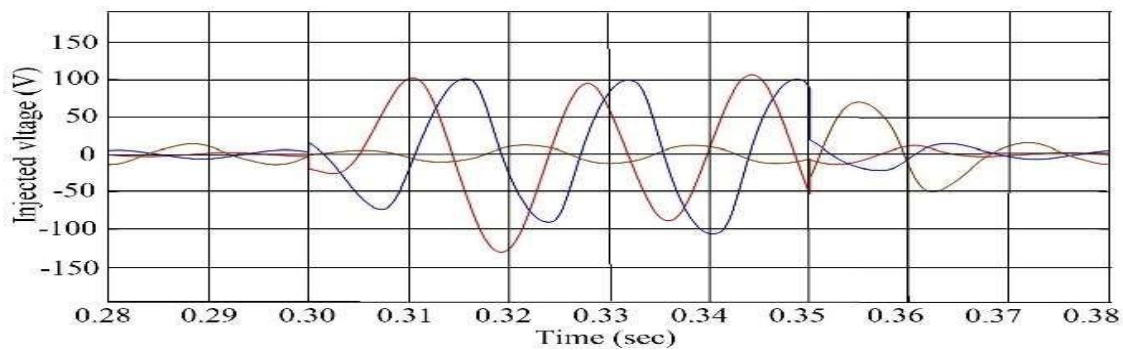
13(b) Injected voltage of DVR



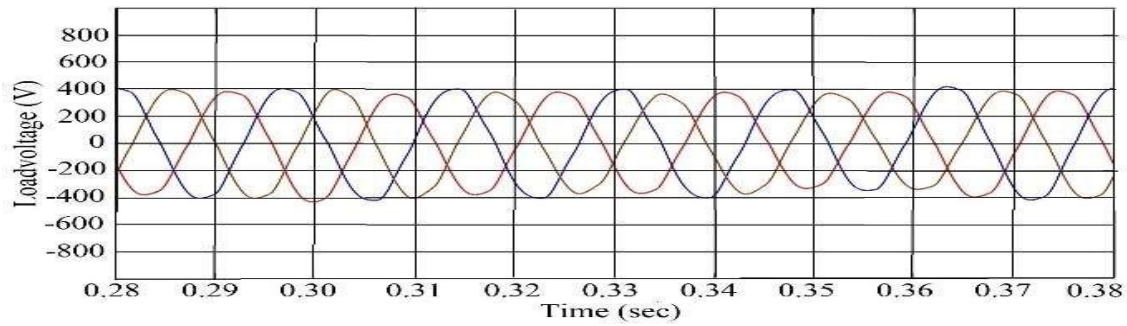
13(c) Load voltage with DVR

Figure 13. 12% symmetrical voltage sag case response of DVR

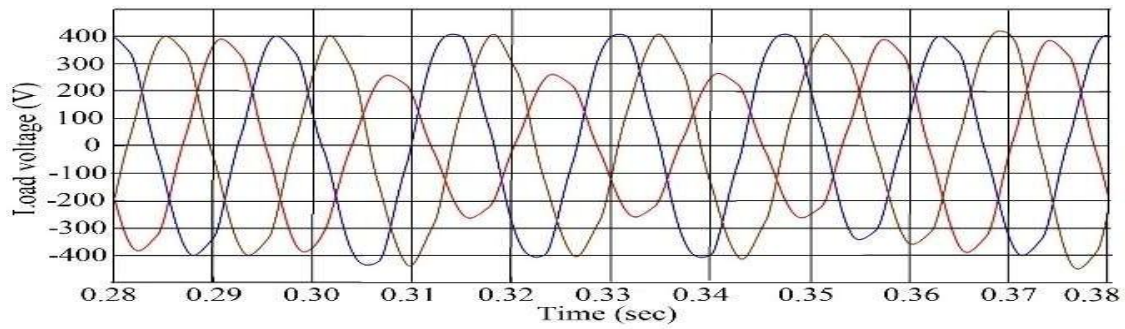
14(a) Load voltage without DVR



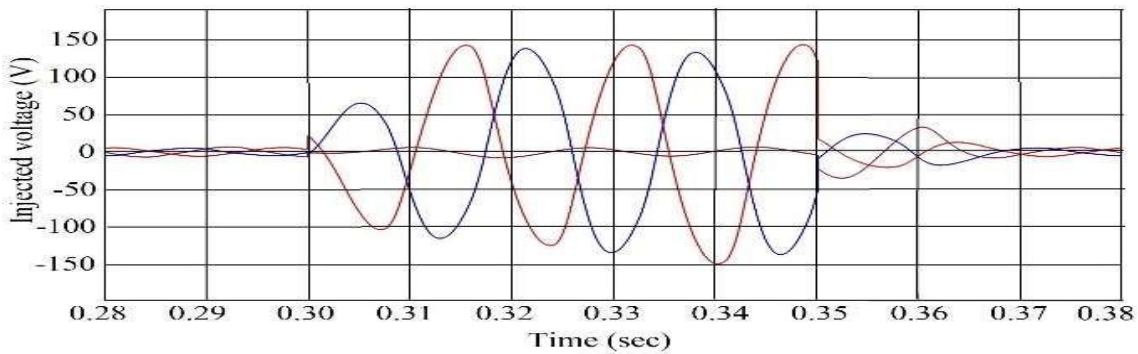
14(b) Injected voltage of DVR



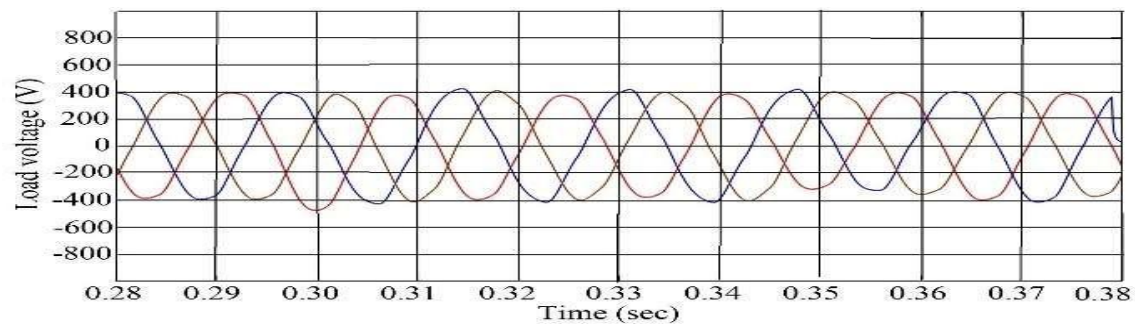
14(c) Load voltage with DVR

Figure 14. 25% asymmetrical voltage sag case response of

15(a) Load voltage without DVR



15(b) Injected voltage of DVR



15(c) Load voltage with DVR

Figure 15. 35% asymmetrical voltage sag case response of

The voltage was dropped not only due to any disturbance, but also due to fluctuations in the source voltage in the hybrid PV-Wind power system connected to grid. In that situation also, the presented BES-SMES based DVR will improve the voltage sag for both symmetrical and asymmetrical cases. The total harmonic distortion (THD) for different voltage sag conditions is shown in Table 4.

Table (4): THD values for different voltage sag cases

Voltage sag case	THD values
25% symmetrical	2.55%
12% symmetrical	4.04%
25% asymmetrical	3.37%
35% asymmetrical	4.39%

6. CONCLUSION

The operation of DVR for grid connected PV-Wind hybrid power system for voltage sag improvement are described. Due to non-linear loads, the faults occurred by the hybrid system, the presented DVR will mitigate these fluctuations. For the proper operation of DVR, the control of BES, SMES and VSC are implemented to identify the voltage level at state of charge (SOC) and point of common coupling. For recovery of both magnitude and phase jumps the pre-sag compensation technique is used. The presented BES-SMES based DVR has three operating conditions, as charging, discharging and energy storing state. The voltage sag improvement of both symmetrical and asymmetrical cases is presented. For 25% and 12% symmetrical voltage sag case the THD will be 2.55% and 4.04%. Similarly, for 25% and 35% asymmetrical voltage sag the THD will be 3.37% and 4.39%. The obtained total harmonic distortion (THD) by fuzzy controller is within the IEEE standards ($\pm 5\%$).

REFERENCES

- [1] BP Statistical Review of World Energy, 68th ed. 2019.
- [2] IRENA, Subsequent of Solar Photovoltaic: Deployment, funding, automation, grid incorporation and socio-economic conditions (The paper is change in universal energy). *International Renewable Energy Agency*, Abu Dhabi, 2019.
- [3] X. Xu, Z. Wei, Q. Ji, C. Wang, and G. Gao, "The evolution of universal renewable energy: Influencing factors, current forecast and achievements," *Resour. Policy*, vol. 63, no. April 2019.
- [4] G. Notton et al., "Irregular and imaginary features of renewable energy sources: Reverberations, irregular cost and welfare of forecasting," *Renew. Sustain. Energy Rev.*, vol. 87, pp. 96–105, 2018.
- [5] S. Agalar and Y. A. Kaplan, "Refinement of power quality to utilize STS and DVR in wind energy system," *Renew. Energy*, vol. 118, pp. 1031–1040, 2018.
- [6] Z. Zheng, X. Xiao, X. Chen, C. Huang, L. Zhao, and C. Li, "Estimation of a MW-Class SMES-BES DVR System for Voltage sag improvement," *IEEE Trans. Ind. Appl.*, vol. 54, no. 4, pp. 3090–3099, 2018.
- [7] A. M. Rauf and V. Khadkikar, "Improvement of Voltage Sag Compensation Techniques for Dynamic Voltage Restorer," *IEEE Trans. Ind. Electron.*, vol. 62, no. 5, pp. 2683–2692, 2015.
- [8] G. Chen, M. Zhu, and X. Cai, "Moderate-voltage level dynamic voltage restorer compensation technologies by positive and negative sequence withdrawal in numerous reference framework," *IET Power Electron*, no. December 2013, pp. 1747–1758, 2014.
- [9] J. Shi et al., "Voltage sag compensations techniques for SMES based dynamic voltage restorer," *IEEE Trans. Appl. Supercond.*, vol. 20, no. 3, pp. 1360–1364, 2010.

- [10] P. F. Ribeiro et al., "Applications of futuristic power in energy storage systems," *ENERGY STORAGE Syst. Adv. POWER Appl.*, vol. 89, no. 12, 2001.
- [11] P. System, W. S. Dvr, Z. Zheng, X. Xiao, C. Huang, and C. Li, "Improvement of short-lived or temporary Voltage Quality in a Distribution Power System With SMES-Based DVR and SFCL," *IEEE Trans. Appl. Supercond.*, vol. 29, no. 2, pp. 1–5, 2019.
- [12] Z. Zheng, X. Xiao, C. Huang, and C. Li, "Improvement of power quality interruptions a kW-Class SMES-BES DVR System is implemented and estimate," *2017 IEEE Int. Conf. Environ. Electr. Eng. 2017 IEEE Ind. Commer. Power Syst. Eur. IEEEIC / I&CPS Eur.*, pp. 1–5, 2017.
- [13] K. Anoune, M. Bouya, A. Astito, and A. Ben, "Sizing methods and optimization techniques for PV-wind based hybrid renewable energy system: A review," *Renew. Sustain. Energy Rev.*, vol. 93, no. June, pp. 652–673, 2018.
- [14] H. Demolli, A. Sakir, A. Ecemis, and M. Gokcek, "Machine learning algorithms for estimating the wind power using daily wind speed data," *Energy Convers. Manag.*, vol. 198, no. July, p. 111823, 2019.
- [15] Y. Han, N. Wang, M. Ma, H. Zhou, S. Dai, and H. Zhu, "A seasonal and nonparametric models for estimating the PV power," *Sol. Energy*, vol. 184, no. April, pp. 515–526, 2019.
- [16] E. M. Molla, C. Liu, and C. Kuo, "Improvement of power quality in wind power plant using microsystem technology," *Microsyst. Technol.*, vol. 26, pp. 1799–1811, 2020.
- [17] K. Basaran, N. S. Cetin, and S. Borekci, "Administration of energy for on-grid and off-grid wind / PV and battery hybrid systems," *IET Renew. Power Gener.*, vol. 11, no. 5, pp. 642–649, 2017.
- [18] F. Barbieri, S. Rajakaruna, and A. Ghosh, "Cloud designing for estimation of PV power: A review," *Renew. Sustain. Energy Rev.*, vol. 75, no. October 2016, pp. 242–263, 2017.
- [19] X. Y. Chen et al., "Contemporary Power System and advanced Smart Grid using integrated SMES methodology," *IEEE Trans. Appl. Supercond.*, vol. 24, no. 5, pp. 1–5, 2014.
- [20] A. K. Sadigh, S. Member, and K. M. Smedley, "Analysis of Voltage Compensation techniques in Dynamic Voltage Restorer (DVR)," *2012 IEEE Power Energy Soc. Gen. Meet.*, pp. 1–8, 2012.
- [21] G. M. As, "Doubly fed induction generator uising back-to-back PWM converters and its application to variable- speed wind energy generation," *IEE Proc.-Electr. Power Appl.*, vol. 143, no. 3, 1996.
- [22] Md. Riyasat Azim, Md. Ashraful Hoque, "A Fuzzy Logic based Dynamic Voltage Restorer for Voltage Sag and Swell enhancement for Industrial application loads" *International Journal of Computer Appl.*, vol. 30, no. 8, 2011.